

[Click to view poster](#)

# Characterization of Sandstones from the *Água Grande* Formation, Recôncavo Basin, Bahia, Brazil, using NMR and Electrical Resistivity

Cristiano Sena<sup>1,2,3</sup>, Joelson da Conceição Batista<sup>1,2,3</sup>, and Luciane Couto<sup>1,2,3</sup>

Search and Discovery Article #42615 (2026)\*\*

Posted March 26, 2026

\*Adapted from extended abstract based on oral presentation given at AAPG International Conference and Exhibition (ICE) Rio de Janeiro, 30 September - 3 October, 2025.

\*\*Datapages © 2026. Serial rights given by author. For all other rights contact author directly. DOI:10.1306/42615Sena2026

<sup>1</sup>Department of Geophysics, Institute of Geosciences (IGEO), Federal University of Bahia (UFBA), Salvador, Brazil

<sup>2</sup>Petrophysics Laboratory (LAPETRO/UFBA)

<sup>3</sup>Study and Application Group for Artificial Intelligence in Geophysics (GAIA/UFBA)

Email: [cristianogomes@ufba.br](mailto:cristianogomes@ufba.br)

## 1. Introduction

The petrophysical characterization of reservoir rocks is essential for assessing their storage capacity, fluid transport behavior, and production potential. These characteristics are influenced by factors such as lithology, porosity, permeability, fluid saturation, clay content, and the architecture and connectivity of pore networks. In addition to conventional well logging, laboratory techniques like Nuclear Magnetic Resonance (NMR) and Electrical Resistivity (ER) measurements have become increasingly valuable. These methods offer direct, non-destructive, and high-resolution insights into pore-scale properties and fluid distribution.

NMR relaxation measurements (e.g.,  $T_2$  distributions) are commonly used to infer pore-size distributions, distinguish between bound and movable fluid fractions, and identify permeability trends (10; 16). Meanwhile, ER measurements, along with Archie-type relationships, remain pivotal for describing electrical transport and estimating fluid saturation. These methods require careful calibration, especially in the presence of heterogeneity and clay-related conduction effects (2; 18). Recently, multiphysics workflows that integrate NMR and resistivity measurements have demonstrated enhanced reliability in estimating pore-throat attributes, capillary pressure behavior, permeability, and saturation levels. This integrated approach helps to reduce uncertainties compared to single-physics interpretations (4; 3).

In this study, we present an integrated NMR–ER methodology to characterize sandstone samples from the *Água Grande* Formation, one of the key hydrocarbon-bearing siliciclastic reservoir units in the Recôncavo Basin of Bahia, Brazil (6).

## 2. Geological Setting

The Recôncavo Basin ([Figure 1](#)), located in eastern Bahia (Brazil), is one of the country's most important onshore sedimentary basins and a classic example of a Jurassic–Cretaceous intracontinental rift system linked to South Atlantic opening and the breakup of Gondwana. Its stratigraphic record is dominated by continental to lacustrine successions (including abundant sandstones and shales) deposited under strong tectonic control, reflecting syn-rift subsidence patterns and fault-controlled sediment dispersal (11; 1). Recognized as Brazil's earliest petroleum-producing province – with the Lobato discovery in 1939 and subsequent early commercial development in the Recôncavo – the basin hosts key reservoir units such as the *Sergi*, *Água Grande*, and *Maracangalha* formations, which remain central targets for geological and geophysical investigation (14).

### 2.1 Location of the Study Area

The *Água Grande* Formation is composed predominantly of fluvial to lacustrine sandstones deposited during the Jurassic – Cretaceous evolution of the Recôncavo rift system. Rock samples were collected from outcrops exposed along the BR-324 highway, representing near-surface analogs of reservoir units at depth ([Figure 2](#)). Although exposed to weathering and ambient temperature – pressure conditions, these outcrop samples are valuable for assessing the petrophysical behavior of this important reservoir formation.

## 3. Methodology

All measurements were conducted at the Petrophysics Laboratory of the Federal University of Bahia (LAPETRO/UFBA). The NMR analyses utilized a modified MARAN Ultra system from Oxford Instruments, operated via the SpecfitLab platform ([Figure 3](#)). Transverse relaxation decay curves ( $T_2$ ) were obtained under conditions of full and irreducible water saturation, enabling the determination of  $T_2$  cut-off values necessary for distinguishing between bound and free fluids. From the acquired CPMG decay signals, inverse Laplace transform (ILT) algorithms were employed to generate  $T_2$  distributions and classify pore size domains. Porosity and permeability estimates were derived using the Timur – Coates model (16), incorporating parameters such as the free-fluid index (FFI), the bound-fluid index (BFI/BVI), and the relationship between the irreducible and fully saturated  $T_2$  components.

Electrical resistivity measurements were obtained using the ARS300 system from Core Laboratories ([Figure 3](#)). The experiments were conducted at various salinity levels to enhance the understanding of rock–fluid interactions and their effects on conductivity responses. The model developed by Lima and Niwas (2000) (7) was utilized to estimate effective porosity, formation factor, and permeability by examining the relationships among bulk conductivity, pore-fluid conductivity, and matrix resistivity. Regression analyses were carried out to assess the correlation between the measured and theoretical conductivity curves.

### 3.1 Fundamental Equations

Petrophysical properties were quantified from laboratory NMR and electrical-resistivity measurements using a set of relationships that connect

the observed physical responses (transverse relaxation and electrical conductivity) to storage and flow attributes. First, a relative NMR-derived porosity was computed from partitions of the  $T_2$  relaxation spectrum. As expressed in Eq. (1),  $\phi_{\text{RMN}}$  was defined as the ratio between the integrated amplitude of the spectrum associated with the selected “irreducible/retained” portion,  $T_{2,\text{irr}}$ , and the total integrated amplitude at full saturation,  $T_{2,\text{sat}}$ , reported as a percentage. This type of  $T_2$ -spectrum partitioning and integral-based quantification follows standard NMR petrophysical practice, where relaxation-time distributions are interpreted in terms of pore-size/relaxation regimes and movable versus bound fluids (10; 8).

Permeability from NMR was then estimated with the general form of the Timur – Coates model (Eq. (2)), in which  $k_{\text{NMR}}$  scales with the NMR porosity,  $\Phi_{\text{rmn}}$ , and with the ratio between the *Free Fluid Index* (FFI) and the *Bound Volume Irreducible* (BVI). The FFI/BVI ratio captures the relative dominance of larger, better-connected pore bodies (movable fluid) versus smaller pores and surface-controlled water (bound fluid), thereby acting as a proxy for hydraulic connectivity and flow capacity (16; 5; 8). The exponents  $a'$  and  $b'$  and the scaling factor  $c'$  are empirical parameters and were treated as calibration constants to be adjusted against laboratory-measured permeability for the studied dataset; literature values may provide initial guesses, but calibration is required to account for sample-specific mineralogical and textural effects.

In parallel, permeability was also estimated from electrical measurements using the family of formulations proposed by Lima & Sri Niwas (2000) (7). In this approach, Eq. (3) links the electrical-based permeability,  $k_{\text{ER}}$ , to the effective porosity  $\phi_e$  while explicitly incorporating the conductive contribution of the solid matrix/clay component through  $\sigma_{c,s}$  and the coupling coefficient  $b_e$ . The parameters  $\alpha_0$  and  $q$  control, respectively, the overall scaling and the sensitivity of the relationship to changes in porosity and matrix conduction, whereas the cementation-related exponent  $m$  modulates the porosity dependence of the transport pathways. This structure is particularly relevant for shaly sandstones, where surface and matrix conduction can be significant and can bias Archie-type interpretations if not explicitly represented (7).

To describe the effective electrical conductivity of the composite medium, Eq. (4) was implemented in a Maxwell – Garnett-type mixing framework, yielding  $\sigma_{o,\text{MG}}$  from a porosity-weighted combination of the pore-water conductivity  $\sigma_w$  and the solid/“matrix” conductivity  $\sigma_{cs}$ , governed by the mixing exponent  $m_{\text{MG}}$  (12). Together, Eqs. (1) – (4) define the workflow used to (i) quantify relative NMR porosity from  $T_2$  spectrum partitions, (ii) infer permeability from NMR via FFI/BVI partitioning (Timur – Coates), and (iii) estimate permeability and electrical transport attributes from resistivity data in the presence of matrix/clay conduction.

$$\phi_{\text{RMN}} = \left( \frac{T_{2,\text{irr}}}{T_{2,\text{sat}}} \right) \times 100\%, \quad (1)$$

$$k_{\text{NMR}} = \left( \frac{\Phi_{\text{rmn}}}{c'} \right)^{a'} \left( \frac{\text{FFI}}{\text{BVI}} \right)^{b'}, \quad (2)$$

$$k_{\text{ER}} = \alpha_0 \left( \frac{\phi_e^{m-1+1/q}}{1 + b_e \sigma_{c,s}} \right)^q, \quad (3)$$

$$\sigma_{o,\text{MG}} = \left[ \phi_e \sigma_w^{1/m_{\text{MG}}} + (1 - \phi_e) \sigma_{cs}^{1/m_{\text{MG}}} \right]^{m_{\text{MG}}}. \quad (4)$$

#### 4. Results

NMR measurements provided quantitative estimates of porosity and permeability based on  $T_2$  relaxation behavior under fully saturated and irreducible water conditions. The resulting parameters reflect variations in pore structure and fluid distribution and are summarized through crossplots ([Figure 4](#), [5](#) and [6](#)).

Electrical resistivity (ER) measurements were used to estimate porosity and permeability, providing complementary information on pore connectivity and fluid distribution. The derived parameters are presented through crossplots ([Figure 7](#)).

Crossplots of porosity versus permeability illustrate the relationships between these parameters and help assess the consistency between estimates derived from Nuclear Magnetic Resonance and Electrical Resistivity ([Figure 8](#)). Additionally, the [Table 1](#) summarizes the entire set of porosity, permeability, and supplementary parameters, providing a detailed quantitative basis for comparing and interpreting reservoir quality across the studied samples.

#### 5. Discussion

The petrophysical parameters derived from NMR and ER data reveal a consistent relationship between porosity, permeability, and pore structure across the analyzed samples. NMR porosity values range approximately from 9% to 18% indicating moderate porosity typical of siliciclastic reservoir rocks. In general, NMR-derived porosity tends to be higher than ER porosity, which is expected due to the sensitivity of NMR measurements to hydrogen-bearing fluids within both connected and isolated pore spaces.

The permeability estimates obtained from NMR exhibit significant variability, reflecting differences in pore-size distribution and connectivity. Samples with higher NMR permeability values are associated with larger free-fluid fractions, suggesting a dominance of macropores and better pore connectivity. Conversely, samples with lower permeability values likely reflect a greater contribution of bound fluid, associated with microporosity and tighter pore throats. This behavior is consistent with the interpretation derived from the Timur – Coates framework, in which permeability is strongly controlled by the balance between FFI and BFI/BVI.

Comparisons between NMR and ER-derived permeabilities show noticeable discrepancies in several samples. These differences may be attributed to methodological differences: ER-based estimates are strongly influenced by pore connectivity and fluid saturation conditions, whereas NMR permeability is indirectly inferred from relaxation mechanisms related to pore geometry. Additionally, variations in grain density and mineralogical composition may contribute to the observed dispersion between the two datasets.

Overall, the combined use of NMR and ER data provides complementary insights into the petrophysical behavior of the samples. While ER measurements are effective in capturing bulk porosity and flow-related properties, NMR data offer a more detailed characterization of pore-size distribution and fluid partitioning, which is crucial for understanding reservoir quality.

## 6. Conclusions

The integration of NMR and ER datasets enabled a robust petrophysical characterization of the analyzed samples. NMR measurements proved particularly effective at identifying variations in pore structure and fluid distribution, allowing distinction between bound and free fluids via  $T_2$  relaxation behavior. The resulting porosity and permeability estimates are consistent with expected trends for reservoir sandstones.

Discrepancies between NMR- and ER-derived permeability values highlight the importance of employing multiple techniques to reduce interpretational ambiguities. While ER data primarily reflect effective porosity and connected pore networks, NMR data provide additional sensitivity to pore-scale features that directly impact fluid storage and mobility.

The results demonstrate that combining NMR analysis with ER data enhances the reliability of petrophysical interpretations, especially in heterogeneous reservoirs. This integrated approach contributes to a more comprehensive assessment of reservoir quality and supports improved predictions of fluid flow behavior in subsurface formations.

## 7. Acknowledgements

The authors thank the Petrophysics Laboratory (LAPETRO) and Federal University of Bahia (UFBA), for infrastructure and technical support during data acquisition and analysis. This work was supported by CNPq (Brazilian National Council for Scientific and Technological Development) through the PIBIC undergraduate research scholarship program

## References

- [1] AAPG (1994). *Recôncavo Basin, Brazil: A Prolific Intracontinental Rift Basin*. In: AAPG Memoir/Edited Volume chapter (Recôncavo Basin overview). AAPG/GeoscienceWorld.
- [2] Archie, G. E. (1942). The electrical resistivity log as an aid in determining some reservoir characteristics. *Transactions of the AIME*, 146 (1), 54–62. doi:10.2118/942054-G.

- [3] Arrieta, D. C., Heidari, Z., Azizoglu, Z., Sahu, P., Nassau, G., Cbncio, P., & Trevizan, W. (2024). Integrated workflow using NMR and electrical resistivity measurements for reliable permeability assessment in vuggy carbonates. In *SPE Annual Technical Conference and Exhibition*. doi:10.2118/221079-MS.
- [4] August, H., Azizoglu, Z., Heidari, Z., et al. (2022). Integrated analysis of NMR and electrical resistivity measurements for enhanced assessment of throat-size distribution, permeability, and capillary pressure in carbonate formations: well-log-based application. In *SPWLA 63rd Annual Logging Symposium*. doi:10.30632/SPWLA-2022-0034.
- [5] Coates, G. R., Xiao, L., & Prammer, M. G. (1991). *NMR Logging: Principles and Applications*. Halliburton Energy Services.
- [6] Cunha, E. C. L., Penna, N. S., & Batista, J. da C. (2019). Petrophysical Analysis of the Água Grande Formation, Recôncavo Basin, Bahia, Brazil. In *Sixteenth International Congress of the Brazilian Geophysical Society (CISBGf)* (Expanded abstract, SBGf).
- [7] de Lima, O. A. L., & Sri Niwas (2000). Estimation of hydraulic parameters of shaly sandstone aquifers from geoelectrical measurements. *Journal of Hydrology*, 235 (1), 12–26. doi:10.1016/S0022-1694(00)00256-0.
- [8] Dunn, K.-J., Bergman, D. J., & LaTorraca, G. A. (eds.) (2002). *Nuclear Magnetic Resonance: Petrophysical and Logging Applications*. Handbook of Geophysical Exploration: Seismic Exploration, Vol. 32. Elsevier.
- [9] Ghignone, J. I. (1970). General Geology and Major Oil Fields of Recôncavo Basin, Brazil. In *Geology of Giant Petroleum Fields*. AAPG Memoir (chapter).
- [10] Kenyon, W. E. (1992). Nuclear magnetic resonance as a petrophysical measurement. *Nuclear Geophysics*, 6 (2), 153–171.
- [11] Magnavita, L. P., Davison, I., & Kusznir, N. J. (1994). Rifting, erosion, and uplift history of the Recôncavo–Tucano–Jatobá Rift, northeast Brazil. *Tectonics*, 13 (2), 367–388. doi:10.1029/93TC02941.
- [12] Maxwell Garnett, J. C. (1904). Colours in metal glasses and in metallic films. *Philosophical Transactions of the Royal Society of London. Series A*, 203, 385–420. doi:10.1098/rsta.1904.0024.
- [13] de Souza Penna, N., da Conceição Batista, J., & Sousa de Vasconcelos, S. (n.d.). RMN e perfis geofísicos de poços na caracterização petrofísica de arenito da formação Maracangalha, Bahia, Brasil. *Revista de Geociências do Nordeste*.
- [14] Rodriguez, M. R., & Suslick, S. B. (2009). An Overview of Brazilian Petroleum Exploration Lease Rounds: history and perspectives. *Terræ Didática*, 6 (1), 3–16.
- [15] Schurr, J. H. (2015). *Physical Properties of Rocks: Fundamentals and Principles of Petrophysics*. 2nd ed. Elsevier.

- [16] Timur, A. (1969). Pulsed Nuclear Magnetic Resonance Studies of Porosity, Movable Fluid, and Permeability of Sandstones. *Journal of Petroleum Technology*, 21 (6), 775–786.
- [17] Xiao, L., Dunn, K.-J., & Heaton, N. (2016). *Nuclear Magnetic Resonance Logging: Principles and Applications*. Elsevier.
- [18] Zhang, P.-J., Pan, B.-Z., Guo, Y.-H., Zhang, L.-H., Si, Z.-W., Xu, F., Zhu, M.-Y., & Li, Y. (2025). Study on an improved saturation parameter method based on joint inversion of NMR and resistivity data in porous media. *Petroleum Science*. doi:10.1016/j.petsci.2025.03.024.
- [19] SOUZA, Lucy; CAMPOS, Diogenes. New Crocodyliiform specimens from Recôncavo-Tucano Basin (Early Cretaceous) of Bahia, Brazil. *Anais da Academia Brasileira de Ciências*, v. 91, 2018. DOI: 10.1590/0001-3765201720170382.

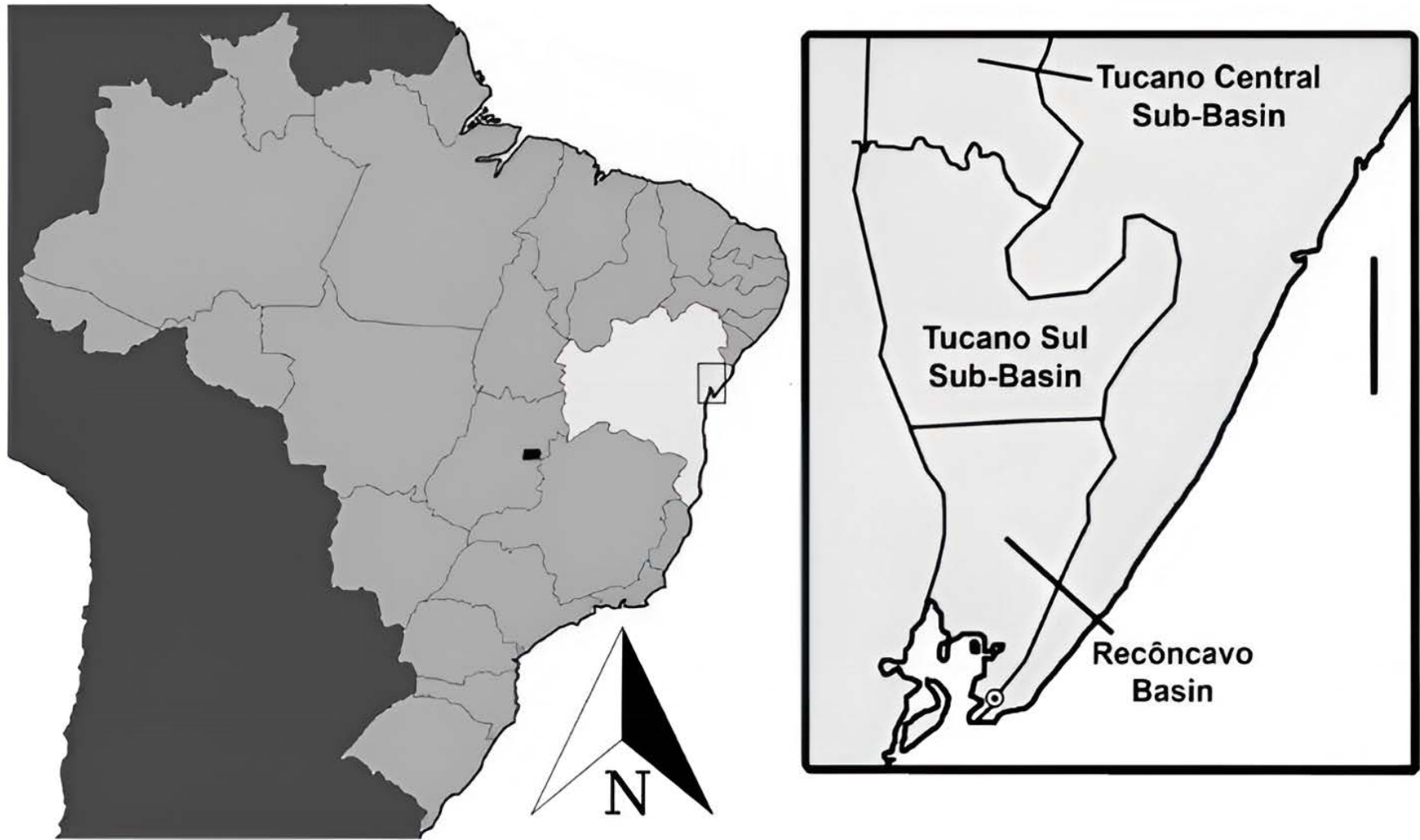


Figure 1. Location and structural framework of the Recôncavo Basin, showing basin subdivision and main fault systems. Source: Modified from Souza & Campos (2018).



Figure 2. Outcrop sampling and resized samples.



Figure 3. Specfit/Maran Ultra NMR (left) and ARS300 equipment (right).

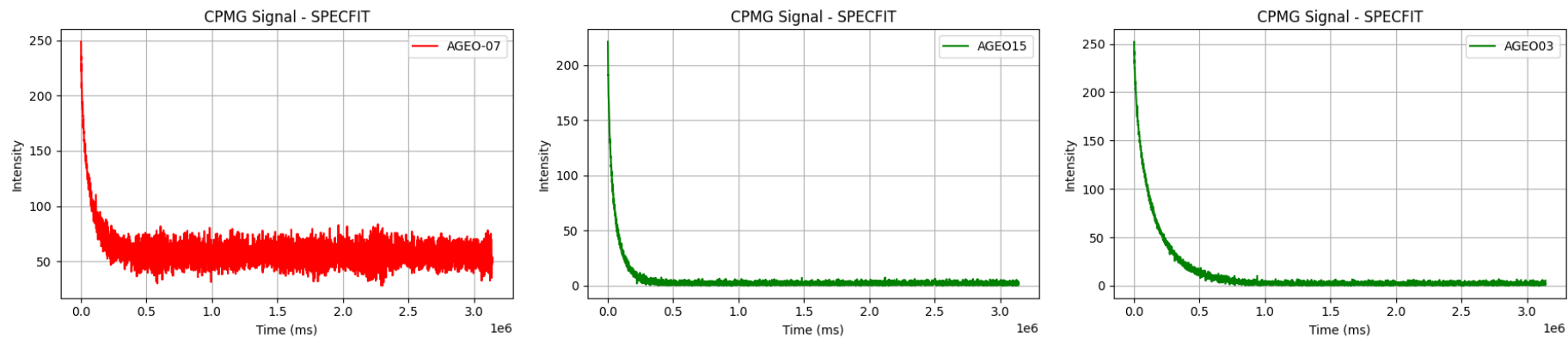


Figure 4. CPMG  $T_2$  decay curves from NMR measurements for representative samples.

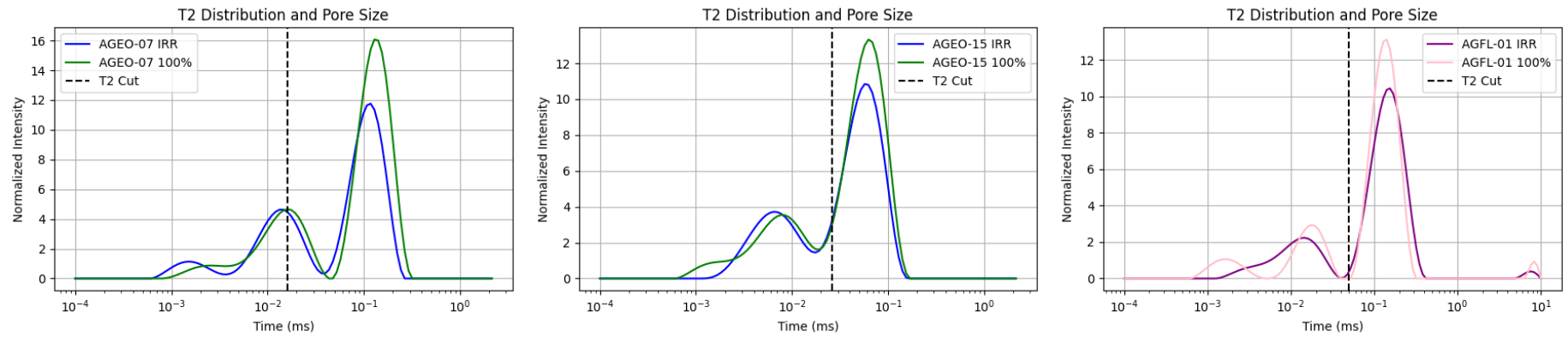


Figure 5.  $T_2$  distributions for representative samples under fully saturated and irreducible water conditions, with the dashed line indicating the  $T_2$  cut-off between bound and free fluids.

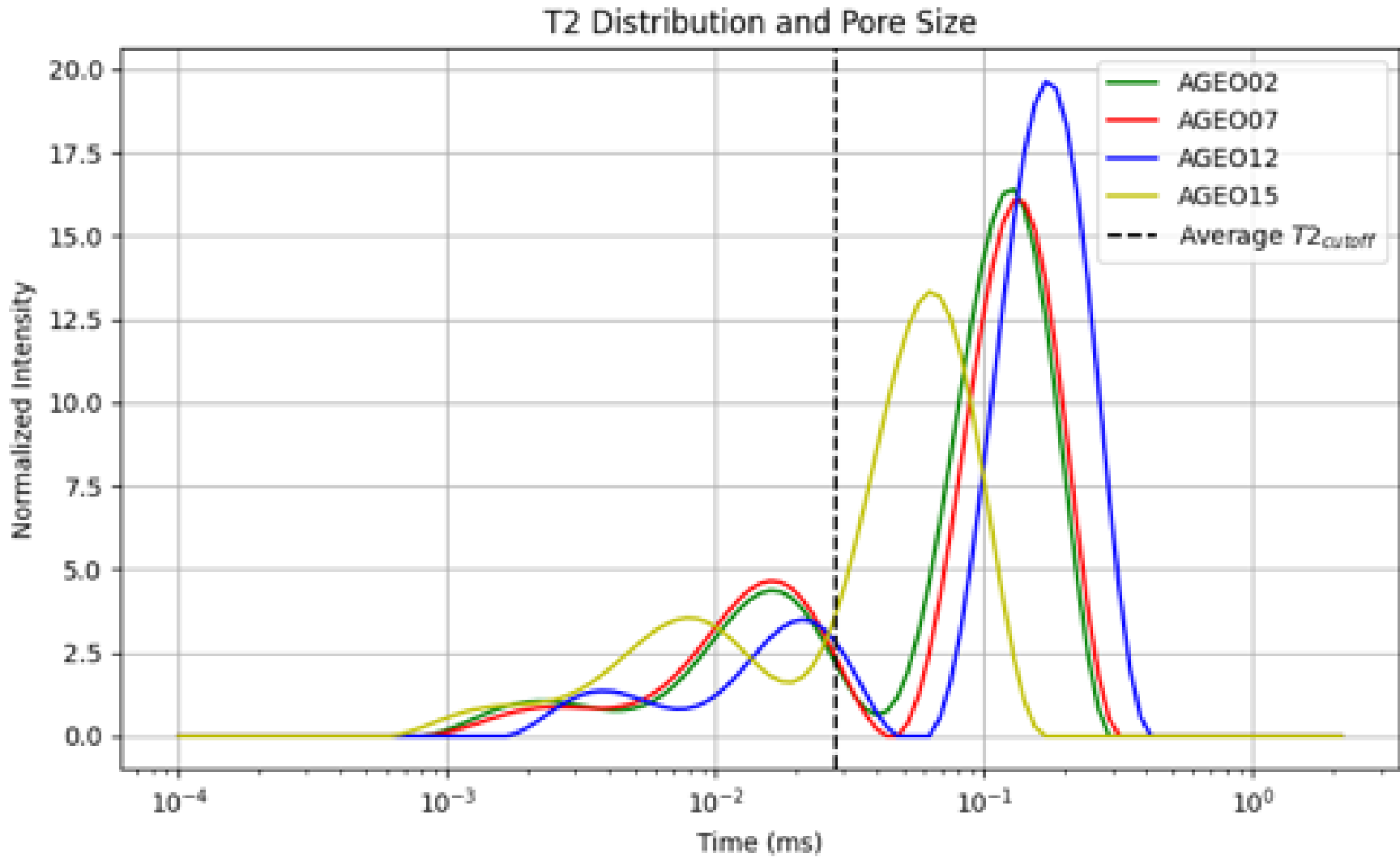


Figure 6. Inverse Laplace transform applied to the CPMG signal to obtain the  $T_2$  distribution and estimate pore size for selected samples.

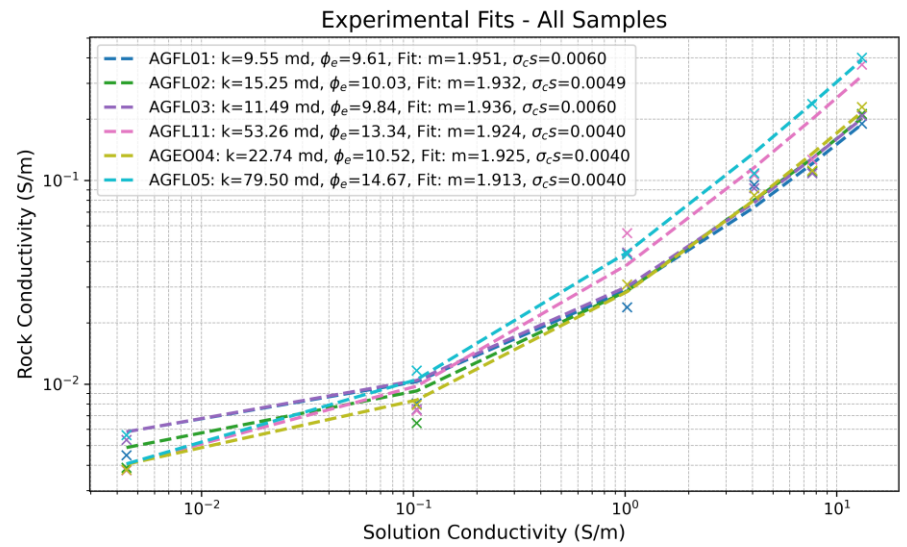
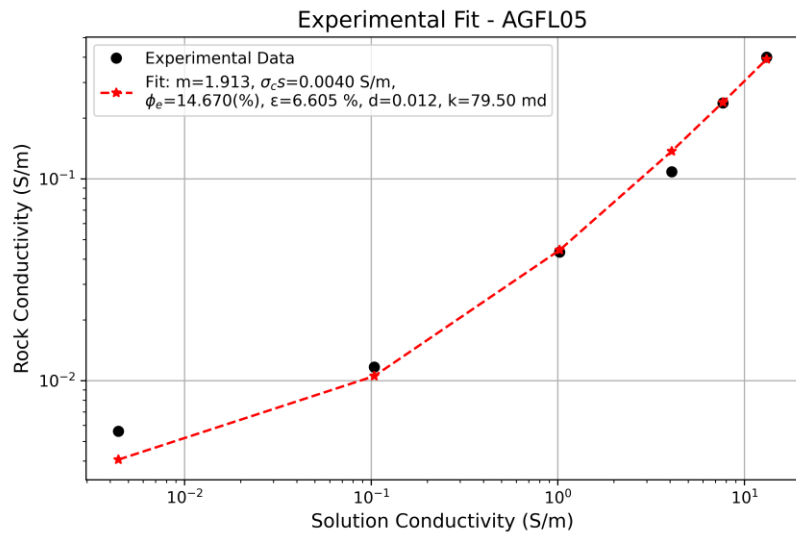
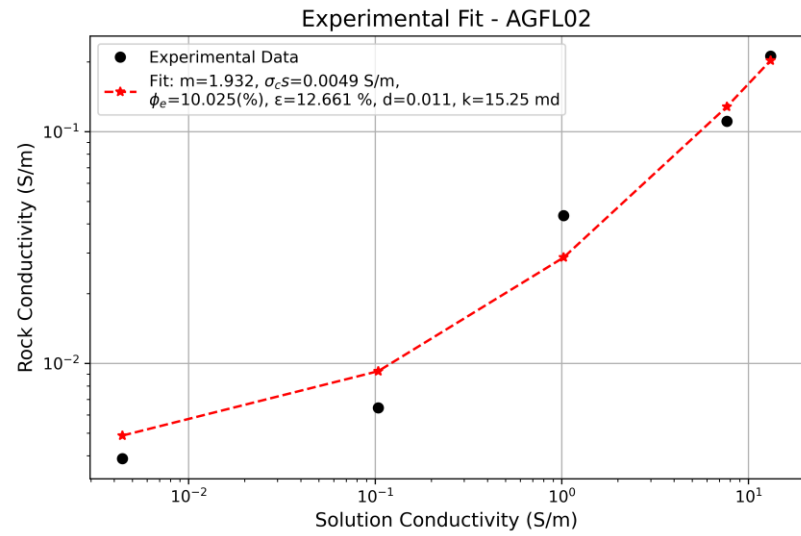
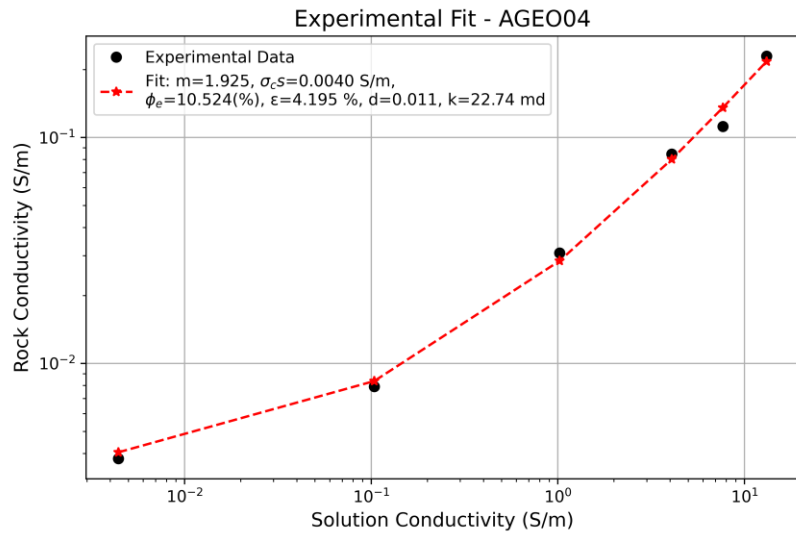


Figure 7. Experimental fits of solution and rock conductivity.

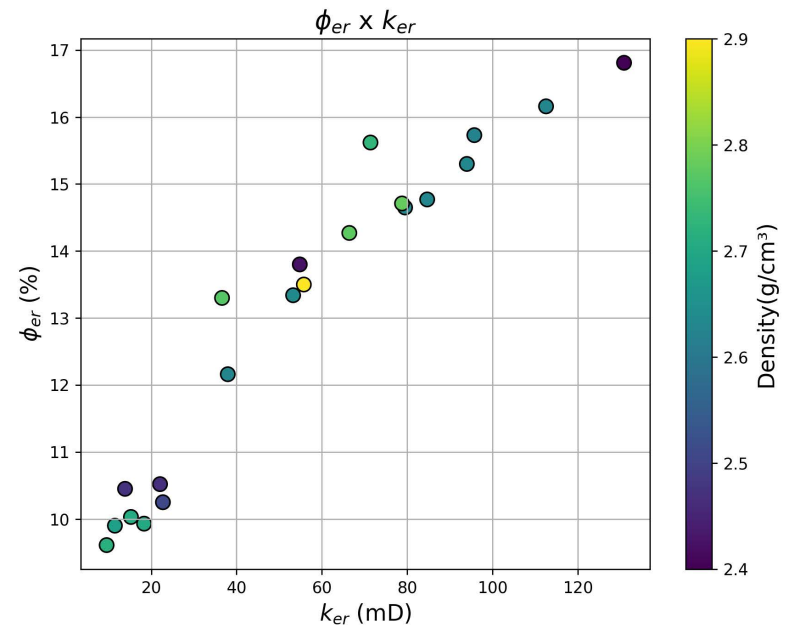
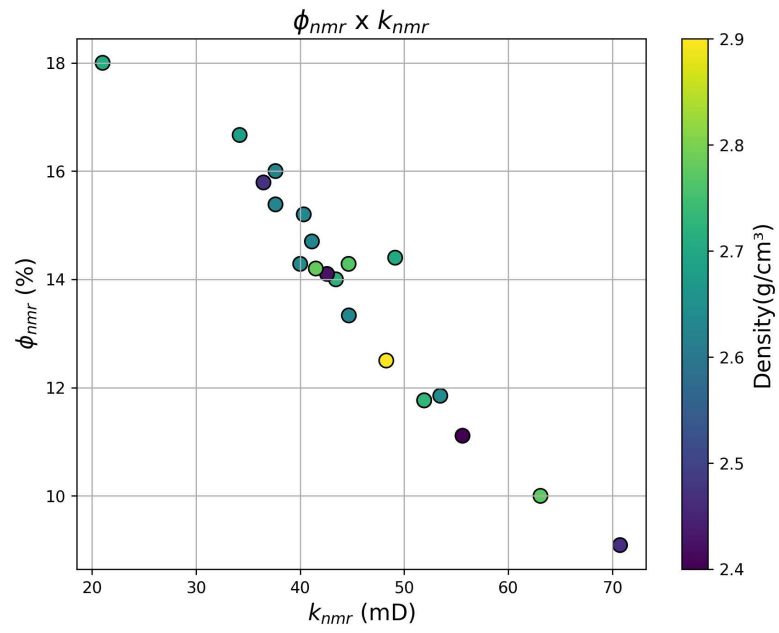


Figure 8. Porosity–permeability dispersion for petrophysical characterization.

Sample	NMR Porosity (%)	NMR Permeability (mD)	Density (g/cm <sup>3</sup> )	ER Porosity (%)	ER Permeability (mD)
AGEO-02	15.38	37.63	2.63	12.16	22.07
AGEO-04	11.76	51.92	2.51	10.25	71.39
AGEO-05	15.79	36.47	2.47	10.45	36.60
AGEO-06	12.50	48.27	2.90	13.50	93.98
AGEO-08	10.00	63.10	2.78	14.27	112.54
AGEO-09	9.09	70.74	2.47	10.52	36.60
AGEO-12	11.76	51.92	2.73	15.62	71.39
AGEO-14	14.70	41.13	2.63	16.16	112.54
AGEO-15	14.29	44.65	2.77	13.30	36.60
AGEO-16	15.20	40.34	2.63	15.30	93.98
AGFL-01	14.00	43.43	2.72	9.61	9.55
AGFL-02	18.00	21.01	2.71	10.03	15.25
AGFL-03	16.67	34.18	2.68	9.90	11.49
AGFL-05	11.85	53.46	2.64	14.65	79.50
AGFL-06	11.11	55.60	2.40	16.81	130.82

Table 1. Petrophysical parameters estimated from NMR and ER data.